https://ntrs.nasa.gov/search.jsp?R=20080034486 2019-08-30T05:21:21+00:00Z

A Grid Sourcing and Adaptation Study Using Unstructured Grids for Supersonic Boom Prediction

Melissa B. Carter * and Karen A. Deere †
NASA Langley Research Center, Hampton, VA 23681

NASA created the Supersonics Project as part of the NASA Fundamental Aeronautics Program to advance technology that will make a supersonic flight over land viable. Computational flow solvers have lacked the ability to accurately predict sonic boom from the near to far field. The focus of this investigation was to establish gridding and adaptation techniques to predict near-to-mid-field (<10 body lengths below the aircraft) boom signatures at supersonic speeds using the USM3D unstructured grid flow solver. The study began by examining sources along the body the aircraft, far field sourcing and far field boundaries. The study then examined several techniques for grid adaptation. During the course of the study, volume sourcing was introduced as a new way to source grids using the grid generation code VGRID. Two different methods of using the volume sources were examined. The first method, based on manual insertion of the numerous volume sources, made great improvements in the prediction capability of USM3D for boom signatures. The second method (SSGRID), which uses an a priori adaptation approach to stretch and shear the original unstructured grid to align the grid and pressure waves, showed similar results with a more automated approach. Due to SSGRID's results and ease of use, the rest of the study focused on developing a best practice using SSGRID. The best practice created by this study for boom predictions using the CFD code USM3D involved: 1) creating a small cylindrical outer boundary either 1 or 2 body lengths in diameter (depending on how far below the aircraft the boom prediction is required), 2) using a single volume source under the aircraft, and 3) using SSGRID to stretch and shear the grid to the desired length.

Nomenclature

p	=	pressure
p_∞	=	free-stream pressure
$\Delta p/p$	=	$(p-p_\infty)/p_\infty$
h/l	=	distance below the model normalized by model length (or body length)
x	=	distance in the stream wise direction, inches

I. Introduction

The desire to transport people and material at velocities greater then the speed of sound has led to considerable research by both industry and the government. In the 1990's, NASA's High-Speed Research Program (HSR) made numerous advances in the areas of aerodynamics and sonic boom.[1,2] In the 2000's, the Super 10 consortium of airframers identified the reduction of sonic boom over-pressures on the ground as a key element to making a viable supersonic business jet.[3] With the creation of the Supersonic Project as part of NASA's Fundamental Aeronautics Program, sonic boom modeling again became a priority. The prediction of the intensity of the sonic boom has usually been computed by obtaining a near-to-mid-field (<10 body lengths below the aircraft) pressure distribution ($\Delta p/p$) and extending it to ground level using atmospheric propagation methods.[4] Using unstructured grids, where it can be difficult to control the distribution and orientation of the field grid beneath the model, pressure signatures in the mid-field typically are insufficiently predicted. Improved results have been obtained using an error-driven adjoint-based grid adaptation method[5,6], but multiple runs using the flow and adjoint solvers can make the process cumbersome. Several hybrid methods[7,8] have been developed that use overset or unstructured grids to compute the

* Aerospace Engineer, Configuration Aerodynamics Branch, MS 499, AIAA Senior Member.
† Aerospace Engineer, Configuration Aerodynamics Branch, MS 499, AIAA Senior Member.

very near-filed solution, then use these results as boundary conditions for a structured grid case that extends into the mid field. While these methods have also been successful, their complexity has motivated research on other methods.

At the beginnning of fiscal year 2007, the state of art for boom prediction using USM3D was from a sourcing method produced by Wyle Labs in 2004 under NASA contract NAS1-98100. This grid sourcing method, shown in figure 1, involved sources coming from the body at the expected Mach angle and continued into the far field 1 body length below the aircraft. An additional set of line sources were used to form a cylinder around the aircraft with a radius of 1 body length. These sources and their locations, had to be manually calculated and inserted. Figure 2 compares the results from this method with experimental data at 1 and 2.5 body lengths. Since the sourcing is focused to the 1 body length, the computational prediction does an excellent job. However, at 2.5 body lengths, the predicted signature looses crispness and no longer is able to predict the intial shock or the recovery.

Since the state-of-the-art boom prediction method was far from the goal of NASA's supersonic program to predict boom up to 10 body lengths below the aircraft, grid sourcing and adaptation methods needed to be significantly improved. This paper details the study of grid sourcing and adaptation to obtain accurate near-to-mid field pressure signatures of supersonic configurations using the computational fluid dynamics (CFD) code USM3D. The study first examines body and far field sourcing, and the shape and sourcing of the outer grid boundaries. From there, several grid adaptation methods are evaluated. Finally, with the recent addition of volume sourcing in the grid generation code, VGRID, two different volume-sourcing techniques are evaluated. This study was conducted using two NASA configurations.[9,10] These two configurations, shown in figure 3, consisted of a simple cone-cylinder, and a generic NASA wing body configuration called the Straight Line Segmented Leading Edge model (SLSLE).

II. Computational Code Information

This computational fluid dynamics (CFD) study used the NASA Tetrahedral Unstructured Software System (TetrUSS[11]) for all the computations. This CFD suite, created and maintained by NASA Langley Research Center, includes an unstructured grid generation program called VGRID, a postprocessor named POSTGRID, and the flow solver USM3D.

VGRID is an interactive, or batch, tetrahedral unstructured grid generation program. The grids produced by VGRID are suitable for computing Euler or Navier-Stokes flow solutions. The grid spacing is related to the strength of user-defined sources placed in the domain. The methodology is based on the Advancing-Front method (AFM)[12] and the Advancing-Layers method (ALM).[13] Both techniques are based on marching processes in which tetrahedral cells grown on an initial triangular boundary mesh and gradually form in the field around the geometry. Once the advancing front process is completed in VGRID, an additional post-processing step is required using POSTGRID to close any open pockets and to improve grid quality.

The USM3D code[14] is a cell-centered, finite-volume Navier-Stokes flow solver that uses Roe flux-difference splitting[15] to compute inviscid flux quantities across the faces of the tetrahedral cells. Several options for turbulent closure are available: the one-equation Spalart-Allmaras (S-A) model[16] (with and without a wall function), and several two-equation models, including Menter's Shear Stress Transport (SST) model.[17] The parallel version of the flow solver was run inviscid and in the implicit mode for the cases presented in this study. The minmod limiter, used for supersonic conditions, was used to ensure during this study to ensure numerical stability.

III. Grid Sourcing

The study began with looking at the initial surface resolution requirements and how to properly source the configuration. Beginning with a basic cone-cylinder configuration, source strength, location and outer boundary shape were examined. The main goal of this study was to determine what type of sourcing would best obtain the peak and recovery pressures since these are typically under predicted by CFD methods

A. Source Size

The goal of this study was to determine the minimum requirements for a surface mesh to capture sonic boom signature. The study began with a baseline mesh that had been created using what, was at the time, best practice sourcing. Variations from the baseline mesh included increasing the number of sources, adding stretching, and changing the source sizes.

The first part of the study looked at global changes. The baseline grid had 11.7 million grid cells and its sourcing is shown in figure 4. Linear sources were used on the body of the configuration while nodal sources were used for the far field. The first grid was produced by reducing all of the sources sizes by 20%, which resulted in a

grid size of 22.7 million cells. A second grid was made by doubling all of the source sizes of the baseline grid, which resulted in a grid size 3.5 million cells. The two grids were run to convergence and the Δp/p results are plotted in figure 5. When compared to the baseline grid, the grid with 3.5 million cells was too coarse and decreased the ability to capture the boom characteristics, while the grid with 22.7 million cells had nearly two times the grid cells and showed only small improvements.

The second part of the study included modifying the body sources, while leaving the far field sources constant. The number of sources along the body and the size of the sources were altered. The different grids tested as part of the body sourcing study on the cone-cylinder configuration, figure 3a, are listed in Table 1. Figure 4 shows the initial sizes of the linear sources on the configuration relative to the nodal sources in the far field. Comparing the changes on Δp/p in figure 6, the 1r and 1u grids resulted in prediction of a strong shock (highest positive or negative Δp/p) which is closer to experimental data (not shown). Although there is very little difference between the results from the two grids, the 1u grid had approximately 18 million more cells than the 1r grid. Therefore, it is important to generate a good surface mesh (1r) to accurately define the configuration, but an ultra-fine surface mesh (1u) only increases the overall volume grid cell count quickly, without further improvements of the sonic boom prediction.

B. Outer Boundary

This part of the study looked at the effect of the outer boundary geometry on Δp/p. The baseline grid's outer boundaries were based on a study conducted by Wyle Laboratories. The outer boundary was a cone with an inner cone removed in order to reduce overall grid size. In both cases, the angle of the cone was based on the shock angle predicted. However, several ideas had been proposed since the study was conducted and it was decided to reexamine the outer boundary geometry.

The first two grids that were tested were altered from the 1r grid (using the baseline outer boundary) by adding back in the second cone and then running the sting to the outer boundary. Please note, that when the sting was added back into the grid, it had to be sourced, there by increasing the grid's overall cell count. The meshes along the symmetry plane for the three grids are shown in figure 7. The boom signatures, Δp/p, at 0.725 body lengths below the model for the three grids are shown in figure 8. Overall the 1r grid with the baseline outer boundary matches the experimental data best with less grid cells than the other two grids analyzed.

The next part of the study looked at the locations of the far field sources. A list all of the grids used in this study, and their grid sizes, are shown in Table 2. Additional sources were added to the baseline sources, along the outer boundaries and in the area of interest (0.725 body lengths below the model). These additional sources are shown in figure 9. The effects of additional sourcing on Δp/p at 0.725 body lengths below the model are shown in figure 10. Results indicate that the 1r grid with baseline outer sourcing matched the experimental data the best. However, the data from adding two sources on each of the outer boundaries was in close correlation with experimental data, with only half the number of cells.

Additionally, an outer box with outer box sourcing strategy was investigated during this part of the study. Figure 11 shows the two outer boundary box and sourcing cases that were analyzed. The outer box sourcing strategies dramatically cut the cell count, as compared with the baseline 1r mesh, see Table 2. The effects of the outer box boundary and box sourcing strategy on Δp/p at 0.725 body lengths below the model are shown in figure 12. The reduced cell count of the outer box strategy dramatically penalized the prediction of boom signature. Here again, the 1r grid with baseline sourcing had the best correlation with experimental data.

IV. Grid Adaptation

After examining grid-sourcing strategies, the study moved toward examining grid adaptation methods. Using the methods from the grid sourcing study, a baseline cone-cylinder and SLSLE grids were produced and then adapted using one of the three methods described below.

A. ADAPT

The ADAPT software[18] is a collection of h-refinement tools in one package, developed by Dr. S. P. Pao of the NASA Langley Research Center. The user can activate one of the three parallel branches of the code for pre-marked cell division; h-refinement in designated spatial domains without a flow solution, adaptive mesh refinement based on functions of the flow solution, or user provided alternate functions. For this study, the adaptive mesh refinement based on pressure coefficient, Cp, was used. Figure 13 shows the results of adapting and refining the grid twice using this code. The first adaptation increased the cell count by 26% while the second adaptation/refinement increased the cell count by an additional 25%. As can be seen, little to no change has been

made on the pressure distribution at a distance of 0.725 and 1.45 body lengths (H/L) below the cone-cylinder configuration.

B. ADV

The ADV adaptation code,[19] by Richard Campbell of the NASA Langley Research Center, grew out of a grid movement method developed to modify an unstructured volume grid after surface design changes were made. In order to provide a grid adaptation capability, a simple approach based on differences in distance and flow variable value between a point and its connected neighbors was implemented. The method has two modes of operation, one that tends to cluster points in regions of high gradient and a second that draws points into zones of high absolute value of the selected flow variable. The second option has been used to provide better wake definitions for high-lift and aeroacoustic computations. A smoothing function can also be invoked to balance the distances to the surrounding points and provide some control over cell aspect ratios. For this part of the study, ADV was used twice: once to produce a grid that just adapted the grids to the area of interest (advc) and the second to both adapt and refine the grid to better capture Cp (adpox). The results from applying ADV on the cone-cylinder configuration are shown in figure 14. The grid produced by adapting the grid had a considerably greater impact than the final grid after refining and adapting the grid.

C. ADAPT/CRISP

An adaptation method using Dr. Paul Pao's ADAPT code and the commercial adaptation code CRISP[20] was suggested by fellow engineers examining boom predictions. CRISP CFD provides an automated grid refinement and coarsening capability. Grid refinement is implemented using a Delaunay procedure where grids of higher density are generated locally in regions where the grid quality fails to meet user specified gradient resolution criteria.

This adaptation method consisted of running ADAPT twice, then running CRISP and finally running ADAPT again. Each time, adaptation was done based on Cp. The original grid, produced by Wyle using the SLSLE model, was used as the baseline case. As shown in figure 15, the predicted boom from the CFD actually deteriorates during the adaptation process. The ability to predict the strength of the initial shock, the strength of the recompression and even the detail in the middle all deteriorate.

In order to ensure that the results weren't due to the original grid already being able to predict the boom signature at 1 body length, another grid was tested using this adaptation method. Using the sourcing techniques from the first part of this study on the SLSLE model, a baseline grid was created and run through the ADAPT/CRISP adaptation method. The comparison of the CFD predicted boom signature with experimental data is shown in figure 16. Although during the process of the adaptation, some improvement was obtained, the CFD prediction was never as close to the experimental results as the Wyle grid without any adaptation.

V. Volume Sourcing

During the course of this study, a new version of VGRID was introduced. Software updates to VGRID included growth rates, surface sources, and volume sources. The outer boundary sources are no longer required for grid growth rates. The outer boundary sources were replaced with a user specified growth rate of the grid that dictates how the grids grow outwards from the aircraft and their maximum size. The new source types available in VGRID are shown in figure 17. In the older version of VGRID, only point and line sources were available. Now, users can define sources that are based on a surface, a sphere, a cylinder or a cone.

With this new capability, researchers looked at the difference in results between anisotropic and isotropic grids. During this study, isotropic refinement methods that add more points in the vicinity of shocks were tested and shown that although they made improvements near the model, they did not necessary improve the pressure signature prediction in the mid-field. This seems to imply that close grid spacing is required normal to the shocks and compression waves to adequately resolve the gradients, but a coarse grid spacing is needed in the propagation direction to minimize the number of cells traversed (and the resulting accumulated dissipation) to reach the mid-field. As a result, two approaches that used stretching of the grid in the shock direction, anisotropic grids, were examined. The first method focused on creating a grid with stretched grid cells aligned with the shocks.[21] The second technique used the SSGRID code[19] to stretch and shear the sources in order to capture the shock. The NASA Straight Line Segmented Leading Edge model (SLSLE) was used for both of these analyses.

A. VGRID Volume Sourcing

The location and set-up of the volumes sources used in VGRID are shown in figure 18, while the grid these sources produced is shown in figure 19. The grid was generated using volume sources that formed the desired grid

and captured the Δp/p without any further alterations to the grid or need for adaptation. The results from this grid are compared with the experimental data and shown in figure 20. This technique predicted the trend and most of the magnitudes in the boom signature, with the exception of the recovery at x=49 inches and the detail between 45 < x < 47 inches. The later exception appears to be the result of a missed geometric detail in the wind tunnel model that was not modeled in the computational mesh. Many researchers, using different codes with the same computational description of the geometry, have missed this same detail

B. SSGIRD

The SSGRID code, created by Richard Campbell of the NASA Langley Research Center, uses a priori adaptation, by which the initial grid is clustered and oriented based on flow characteristics, such as Mach number. A small grid is created around the aircraft of interest, usually with an cylindrical outer boundary with a 1 body length diameter. Underneath the aircraft, a volume source is created that encompasses the length of the aircraft and goes from just underneath it to the lower boundary, as shown in figure 21. Then, the preliminary cylindrical grid, shown in figure 22, is run through SSGRID where the user specifies a desired outer boundary distance (in dimensions of body lengths). The grid points between the preliminary cylinder outer boundary and the desired conical outer boundary are first stretched in a radial direction to a specified distance, then sheared conically to match the free-stream Mach angle. This aligns the stretch direction with the shocks (figure 23) so that only a small flow gradient is encountered in that direction. The comparison of predicted Δp/p with experimental data, at 2.5 body lengths below the SLSLE aircraft, is shown in figure 24. As with the previous method, this technique correlates well with experimental data, with the exception of the recovery at x=49 inches and the detail between 45 < x < 47 inches. The benefits of this technique include small grid sizes and the ability to easily make new grids with different freestream conditions, by simply running SSGRID on the preliminary mesh with new Mach numbers

VI. Further SSGRID Studies

Due to the ease of use of SSGRID and its ability to predict the boom signature, the rest of the study focused on using SSGRID.

A. Sting Modeling

The study now focused on accurately predicting the recompression at the aft of the signature. The first step was to test whether modeling the sting was necessary. Figure 25 compares the boom signatures of the SLSLE with and without the sting modeled using SSGRID. Although no difference is seen in the predicted recompression, by modeling the sting, the second recompression (at x=26) predicted by CFD is removed.

B. Adaptation

Since adaptation was tested with prior gridding techniques, ADV was used to adapt (not adapt and refine) the grid. Grid cells were clustered together based on Cp gradient. Adaptation was tried twice, once to a grid without the sting and once to a grid with the sting modeled. Figure 26 shows that although adaptation doesn't make huge changes to the results, it does better capture the curvature of the initial shock (insert) and predicts a slightly larger recompression in the aft region (from x=164 to x=168) of the signature.

C. Size of Outer Boundary

Since the recompression was still being missed by the CFD predictions, the initial size of the grid produced was examined to ensure the grid cells were not being stretched and sheared too far. A new initial cylindrical grid with a radius of 2 body lengths was produced and using SSGRID stretched to obtain a 10 body length prediction. The results of the 1 body length and 2 body length radius cylinders are compared in figure 27. Additionally, the 2 body length radius cylinder's solution was also adapted using ADV. The larger initial grid was able to predict the recompression and through additional testing, it was determined that a 1 body length radius cylinder could give reasonable boom predictions up to 5 body lengths below the aircraft while 2 body length radius was necessary in order to obtain predictions at 10 body lengths.

VII. Best Practice Conclusion

This paper detailed the sourcing and adaptation study that was conducted for NASA's supersonic program. Although numerous gridding options were examined and adaptation techniques tested, it was the addition of volume

sources in VGRID that permitted accurate boom predictions using the USM3D CFD code. Figures 28 and 29 compare the previously best CFD predictions with results from SSGRID. At 1.5 body lengths below the aircraft, the strength of aft recompression is now predicted. At 10 body lengths, which was not obtainable previously, USM3D using SSGRID can now predict the boom signature strength and details. The best practice created by the study for boom predictions using the CFD code USM3D involves: 1) creating a small cylindrical outer boundary either 1 or 2 body lengths in diameter (depending on how far below the aircraft the boom prediction is required), 2) using a single volume source under the aircraft, and 3) using SSGRID to stretch and shear the grid to the desired length.

References

[1] Wood, R. M.: First NASA/Industry High-Speed Research Configuration Aerodynamics Workshop. NASA/CP-1999-209690-PT1, December 1999.

[2] Edwards, T. A.: High-Speed Research: Sonic Boom, Volume I. NASA-CP-10132, February, 1994.

[3] "Lowering the Boom", The X-Press, NASA Dryden Flight Research Center, Volume 47, Issue 4, July 29, 2005. http://www.nasa.gov/centers/dryden/news/X-Press/stories/2005/072905_LoweringTheBoom.html

[4] Page, J. A.; and Plotkin, K. J.: An Efficient Method for Incorporating Computational Fluid Dynamics Into Sonic Boom Prediction, AIAA 91-3275, 1991.

[5] Jones, W.T.; Nielsen, E.J.; and Park, M.A.: "Validation of 3D Adjoint Based Error Estimation and Mesh Adaptation for Sonic Boom Prediction", AIAA-2006-1150, January 2006.

[6] Park, M. A. and Darmofal, D. L.: Output-Adaptive Tetrahedral Cut-Cell Validation for Sonic Boom Prediction, AIAA-2008-6594, August 2008.

[7] Laflin, Kelly R.; Klausmeyer, Steven M.; and Chaffin, Mark: "A Hybrid Computational Fluid Dynamics Procedure for Sonic Boom Prediction", AIAA-2006-3168, June 2006.

[8] Waithe, Kenrick A.: "Application of USM3D for Sonic Boom Prediction by Utilizing a Hybrid Procedure", AIAA-2008-129, January 2008.

[9] Mack, R. J.; and Kuhn, N: Determination of Extrapolation Distance with Measured Pressure Signatures from Two Low-Boom Models, NASA TM-2004-213264, 2004.

[10] Mack, R. J.; and Kuhn, N: Determination of Extrapolation Distance with Pressure Signatures Measured at Two to Twenty Span Lengths from Two Low-Boom Models, NASA TM-2006-214524, 2006.

[11] Frink,N. T.; Pirzadeh, S.Z.; Parikh, P.C.; Pandya, M.J.; and Bhat, M.K. The NASA Tetrahedral Unstructured Software System, The Aeronautical Journal, Vol. 104, No. 1040, October 2000, pp. 491-499.

[12] Lohner R and Parikh P. Three-dimensional grid generation by the advancing front method. Int.J.Num.Meth. Fluids 8, pp 1135-1149 (1988).

[13] Pirzadeh S. Three-dimensional unstructured viscous grids by the advancing layers method. AIAA Journal, Vol. 34, No. 1, January 1996, pp. 43-49.

[14] Frink, N. T., Three-Dimensional Upwind Scheme for Solving the Euler Equations on Unstructured Tetrahedral Grids, Ph. D. Dissertation, Virginia Polytechnic Institute and State University, September 1991.

[15] Roe, P., Characteristic Based Schemes for the Euler Equations,"Annual Review of Fluid Mechanics, Vol. 18, 1986, pp. 337-365.

[16] Spalart, P.; and Allmaras, S.A.: One-equation turbulence model for aerodynamic flows. AIAA 92-0439, January 1992.

[17] Menter, F.R.: Improved Two-Equation k-omega Turbulence Models for Aerodynamic Flows, NASA TM-103975, October 1992

[18] Frink, N.T. and McMillin, S.N.: CEV/CM CFD Simulation Guidelines for USM3D Navier-Stokes Solver, EG-CAP-06-34 Version 1.03, Aerosciences & Flight Mechanics Division, NASA Lyndon B. Johnson Space Center, Houston, Texas, October 20, 2006.

[19] Campbell, R. C.; Carter, M. B.; Deere, K.A.; and Waithe, K. A.: Efficient Unstructured Grid Adaptation Methods for Sonic Boom Prediction. AIAA-2008-7327, August 2008.

[20] Cavallo, P. A. and Grismer, M. J.: A Parallel Adaptation Package for Three-Dimensional Mixed-Element Unstructured Meshes. AIAA Journal of Aerospace Computing, Information, and Communication. Vol. 2, November 2005, pp. 433-450.

[21] Pirzadeh S.: Advanced Unstructured Grid Generation for Challenging Aerodynamics Applications. AIAA-2008-7178, August 2008.

Mesh	# cone sources	# cylinder sources	X=14 source	TE source	Grid Cell Count(M)
1	2	2	.1	.1	11.7
1o	2	2	.01	.1	14.9
1n	1	2	.01	.1	17.1
1m	1	1	none	.1	2.2
1q	1	2	.01	.05	20.1
1r	1	3	.01	.04	35.8
1u	1	4	.01	.04	53.6

Table 1 Listing of Grids Analyzed While Altering Only the Body Sources

Grids	**Cells**
1 r Grid w/Baseline Outer Boundary	35.8 mil
1 Additional Souce on each outer line	16.1 mil
1 Additional Source on each outer line (refined)	23.5 mil
2 Additional Sources on each outer line	18.8 mil
Region of Interest Sourcing	40.3 mil
Box Grid	8.3 mil
Box Grid (refined)	7.2 mil
Box Grid with Inner Box	3.8 mil

Table 2 Listing of Grids Analyzed While Altering the Outer Boundary

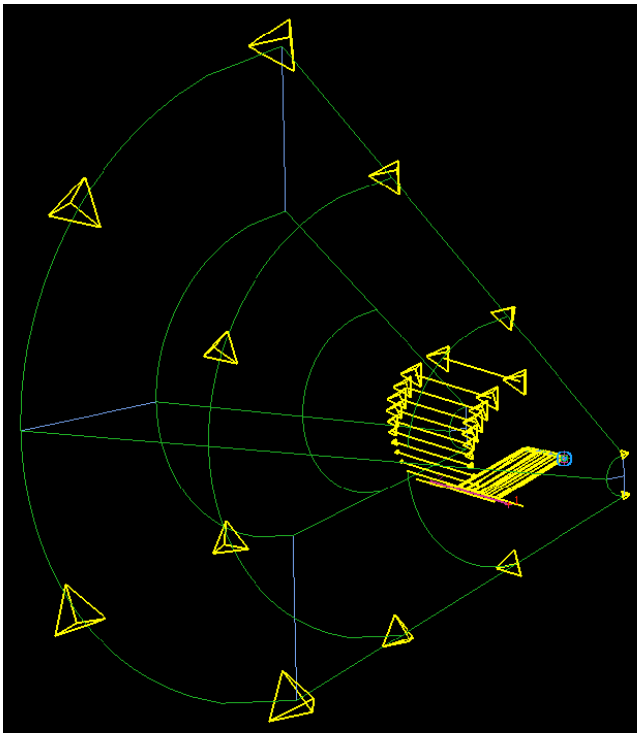

Figure 1 State of the Art Sourcing Technique from Wyle Laboratories

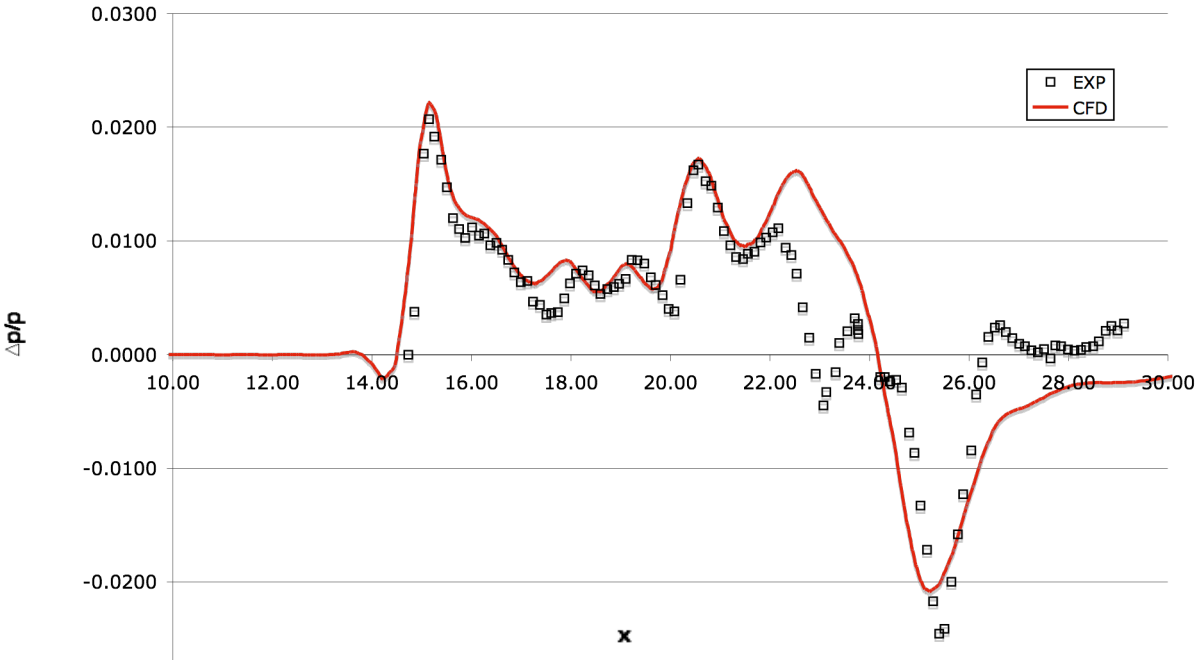

a) 1 Body Length below Model

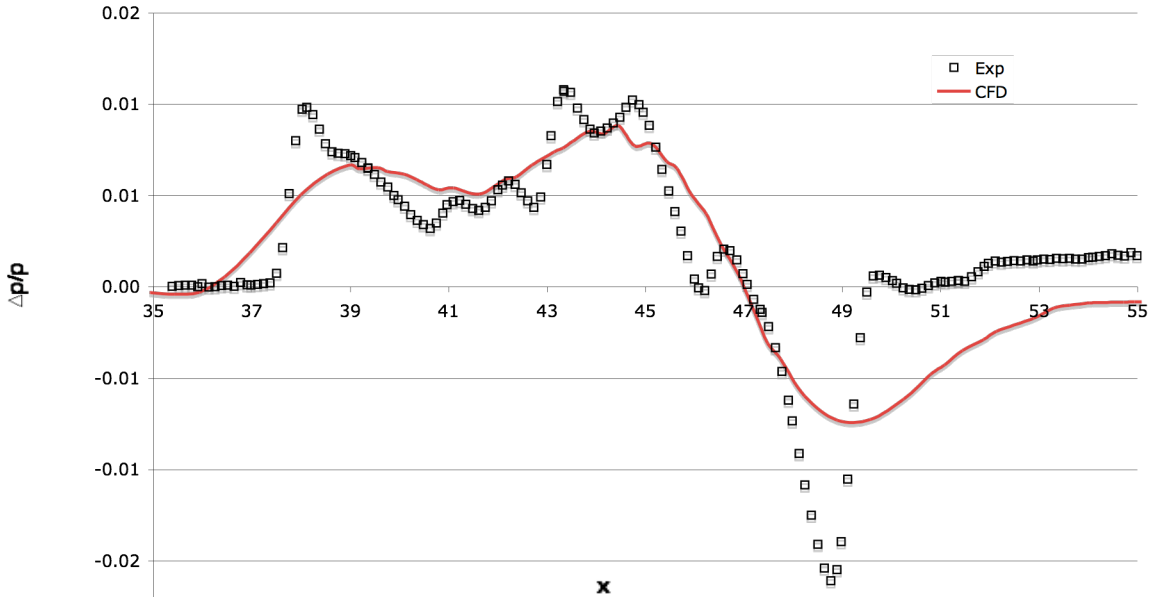

b) 2.5 Body Lengths below Model

Figure 2 Comparisons of Computational Results from Wyle Grid with Experimental Data

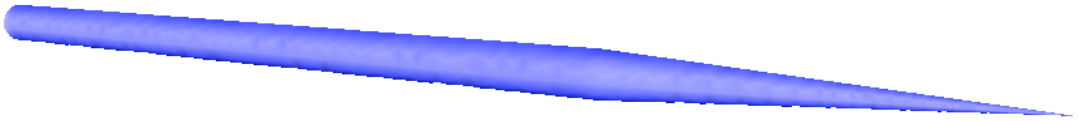

a) Cone Cylinder Model

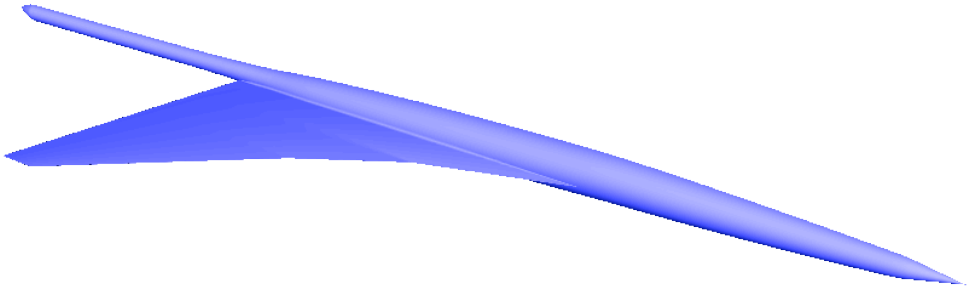

b) Straight Line Segmented Leading Edge (SLSLE) Model

Figure 3 NASA in-house models used in this study

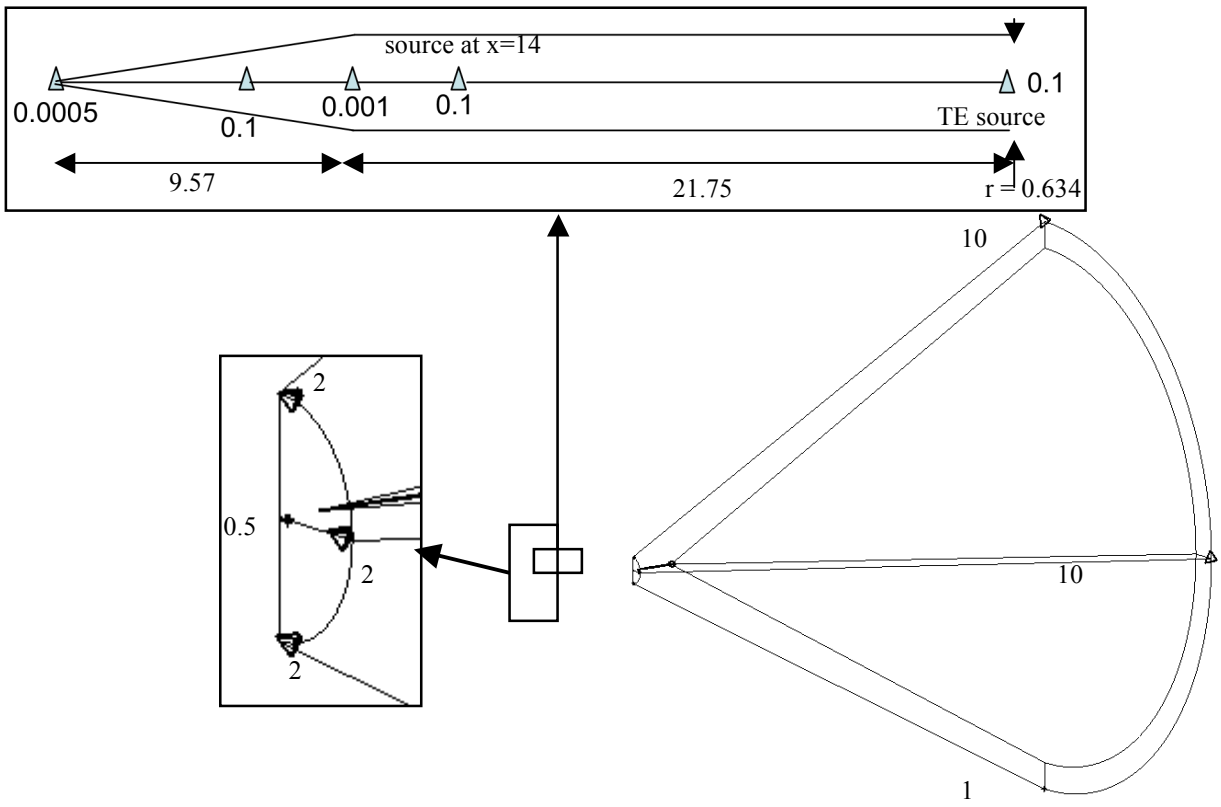

Figure 4 Baseline Sourcing of Cone-Cylinder and Outer Boundary

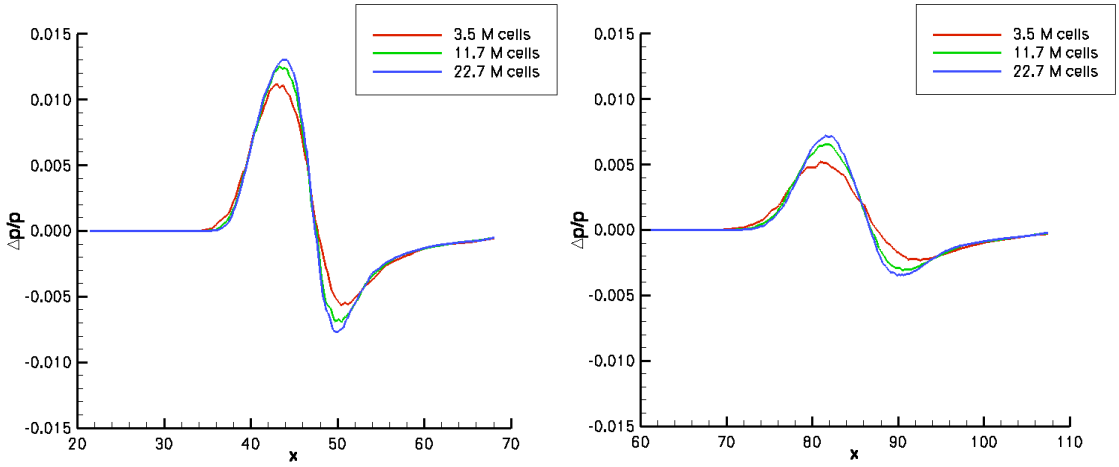

a) 0.725 Body Lengths Below Cone-Cylinder **b) 1.45 Body Lengths Below Cone-Cylinder**

Figure 5 Comparisons of Results from Global Changes on Δp/p

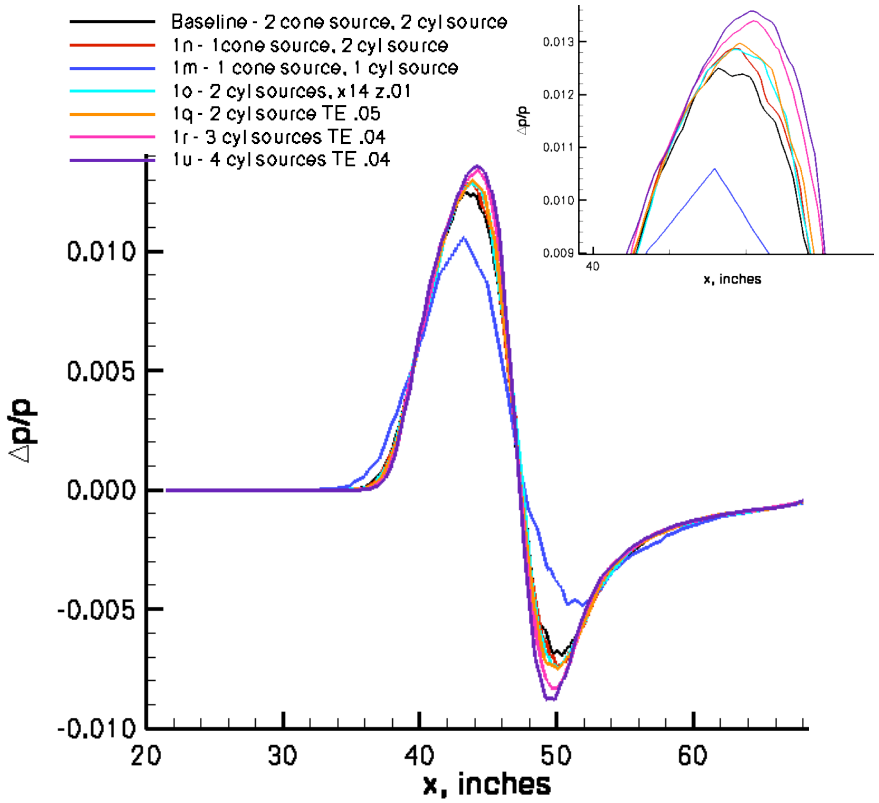

a) 0.725 Body Lengths Below Cone-Cylinder

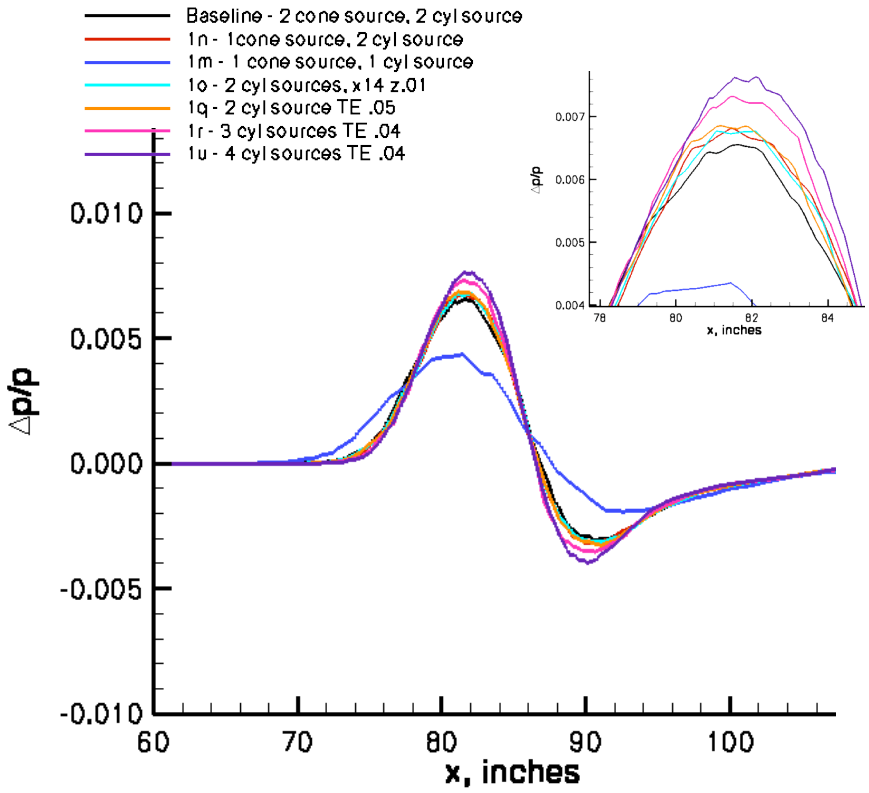

b) 1.45 Body Lengths Below Cone-Cylinder

Figure 6 Comparison of Body Source Effects on Δp/p

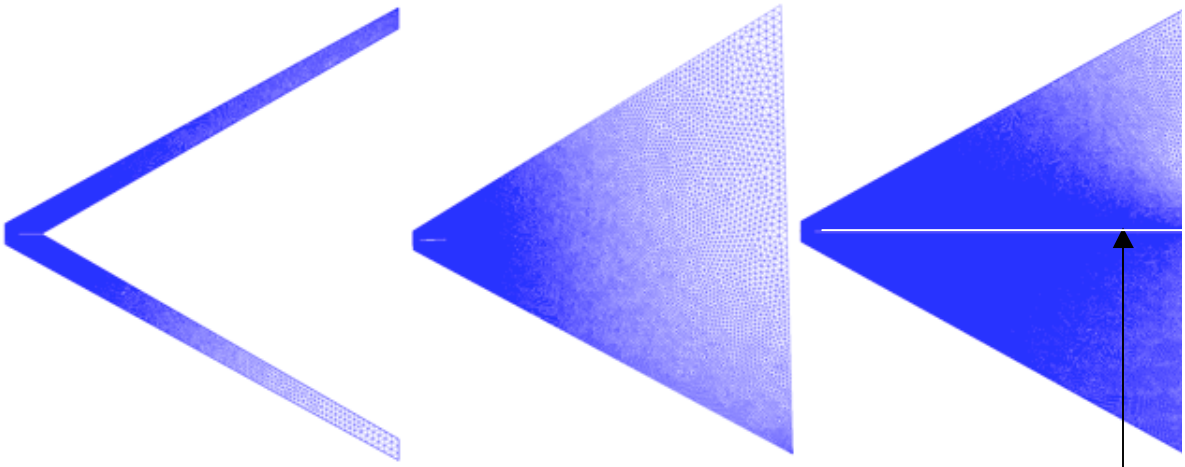

a) Baseline **b) Inner Cone Not Removed** **c) Inner Cone Not Removed and Sting Extended**

Figure 7 Far Field Domains Tested

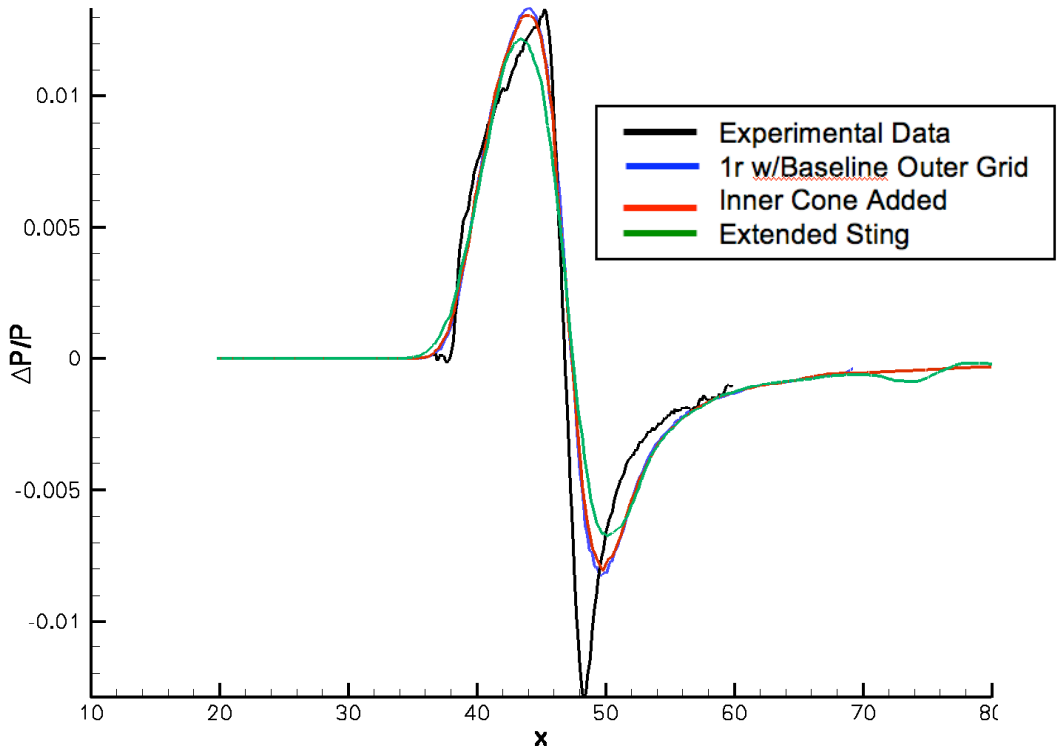

Figure 8 Boom Predictions from Changing Far Field Domain at 0.725 Body Lengths Below Cone-Cylinder

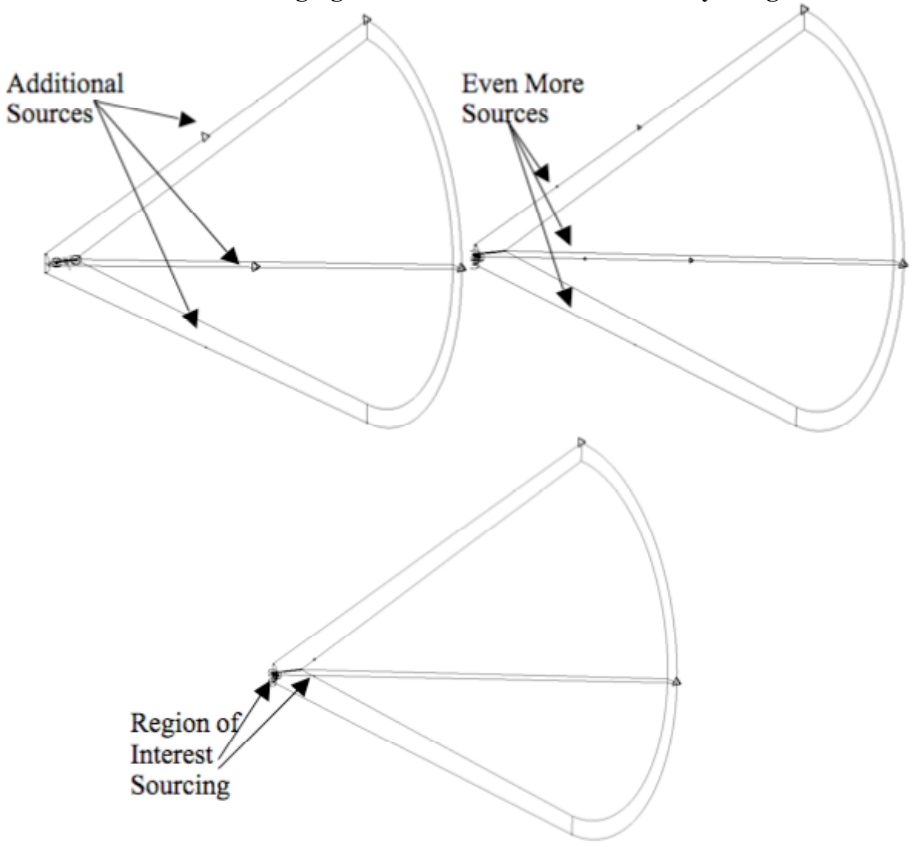

Figure 9 Far Field Sourcing

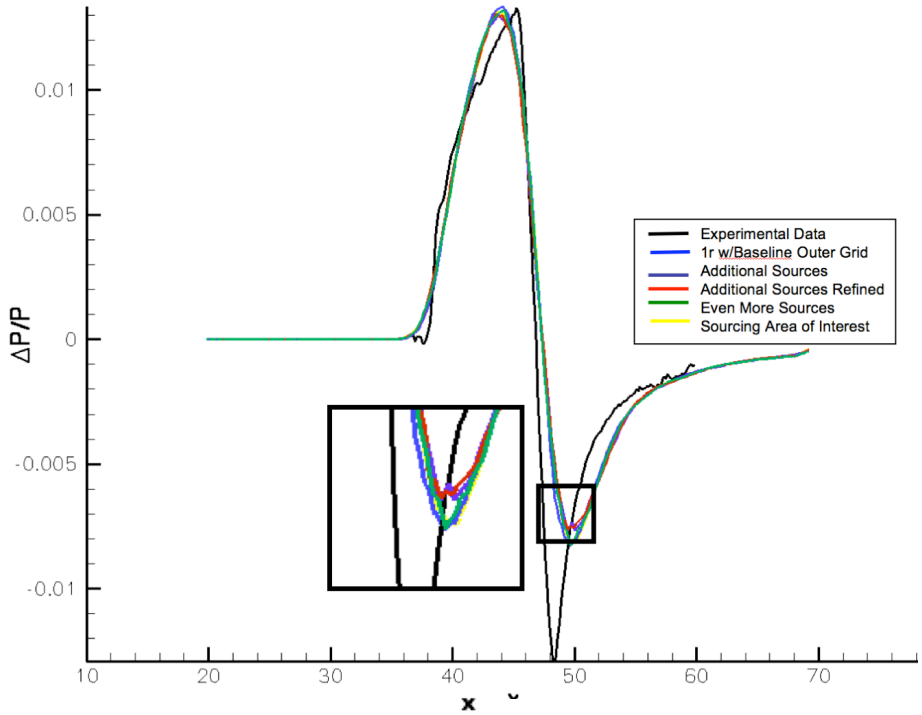

Figure 10 Boom Predictions from Changing Far Field Sourcing at 0.725 Body Lengths Below Cone-Cylinder

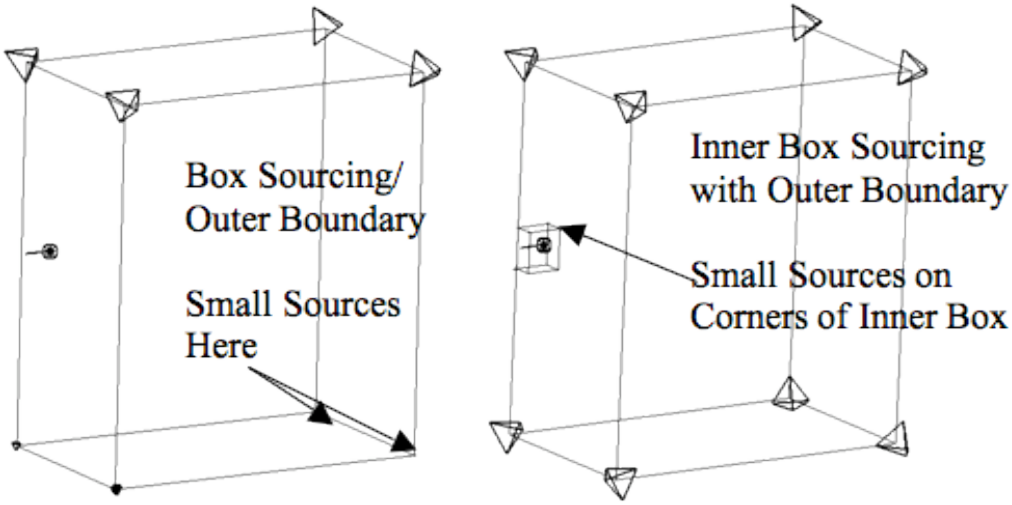

Figure 11 Far Field Box Sourcing

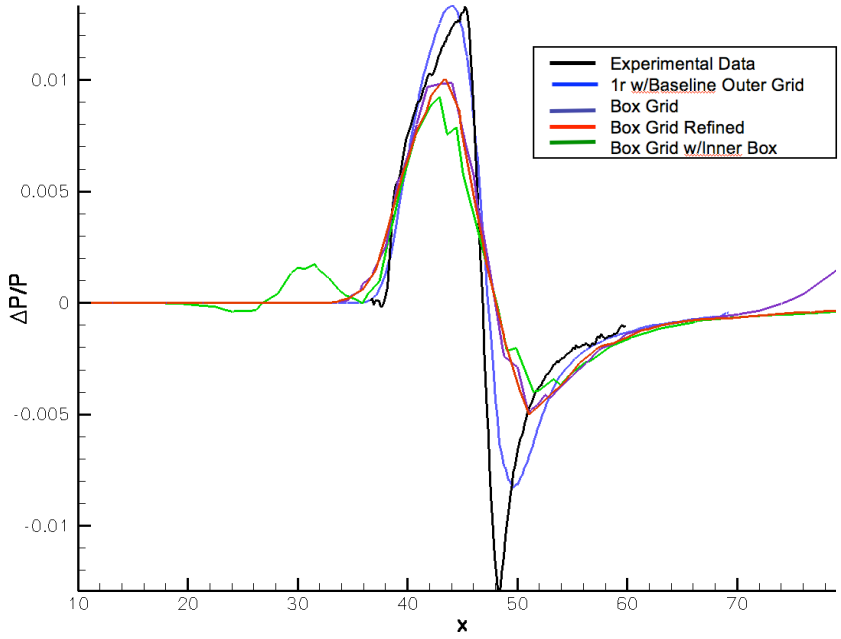

Figure 12 Boom Predictions from Changing Far Field Box Sourcing at 0.725 Body Lengths Below Cone-Cylinder

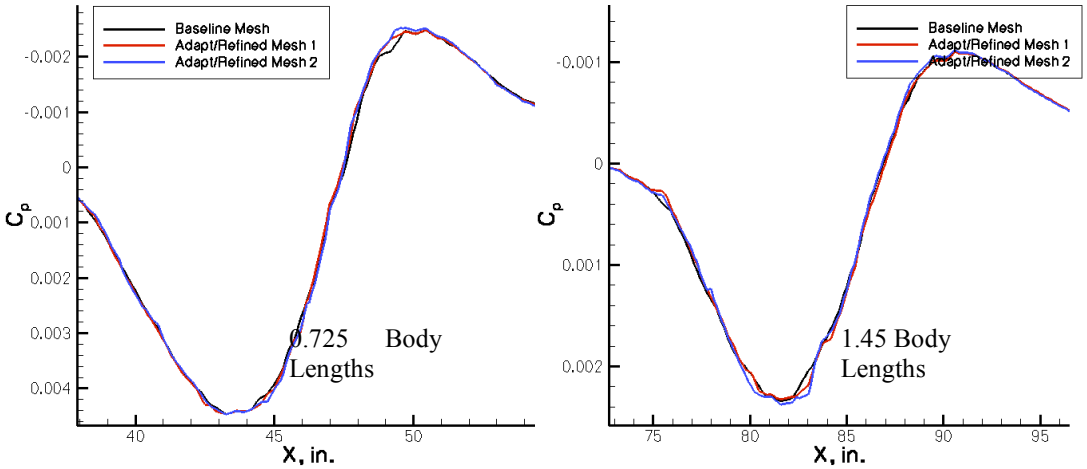

Figure 13 Effects of using ADAPT on Cp Predictions on Cone Cylinder

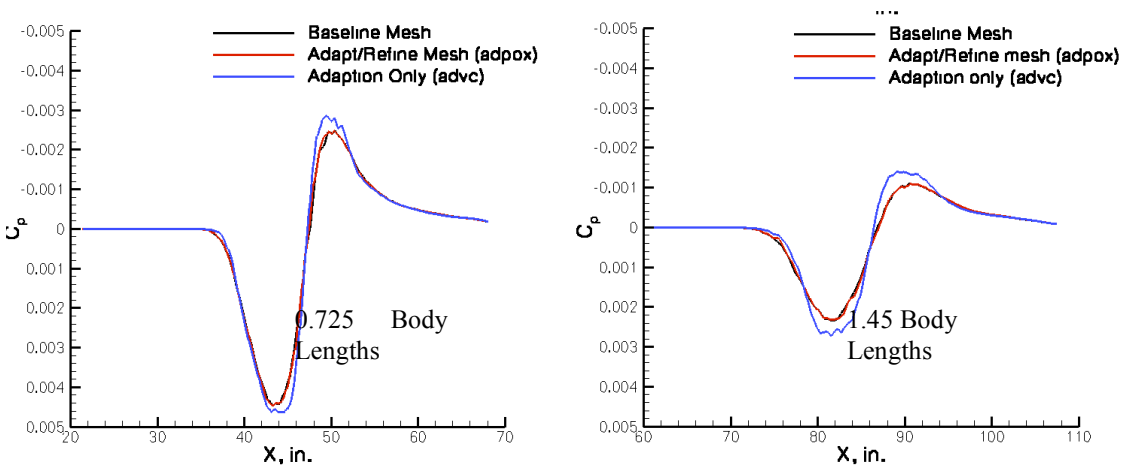

Figure 14 Effects of using ADV on Cp

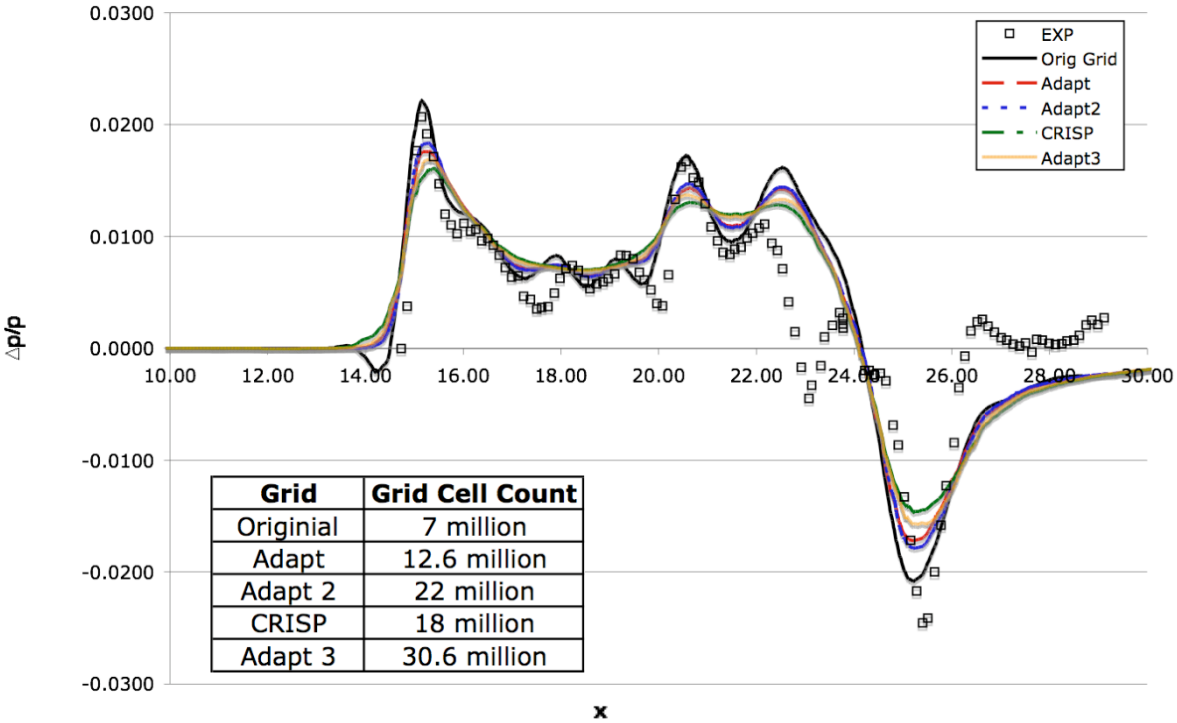

Figure 15 ADAPT/CRISP Adaptation Method at 1 Body Length below SLSLE Process Started with Wyle Grid

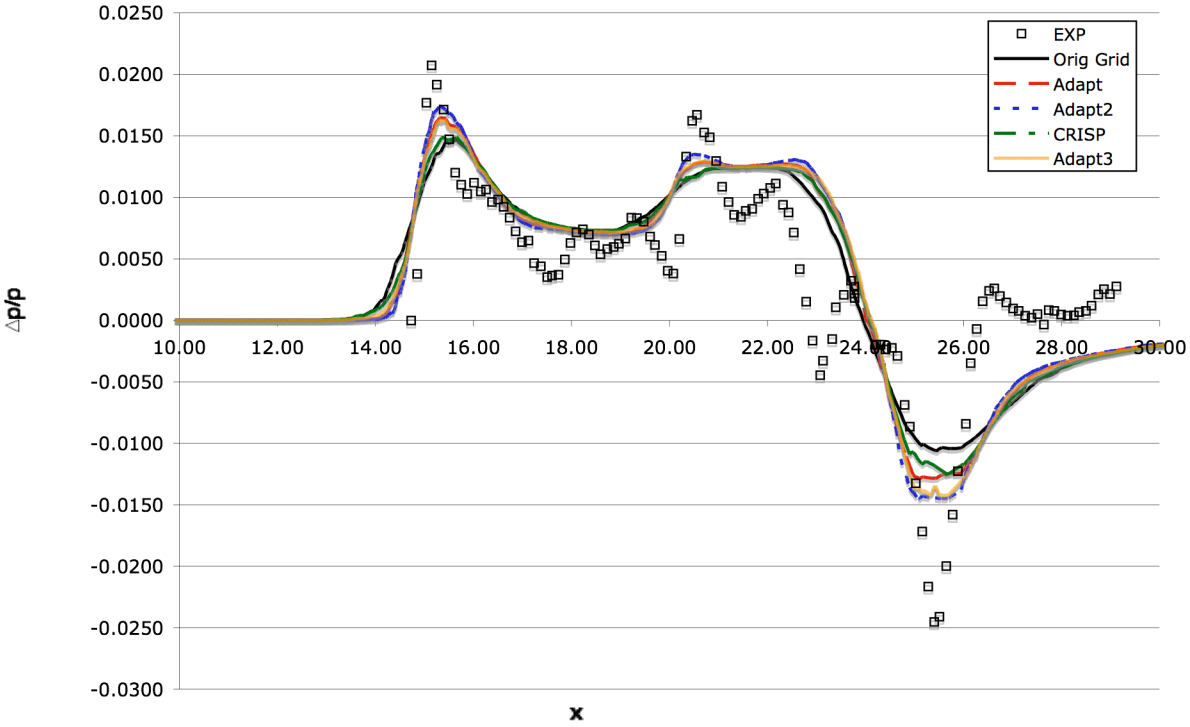

Figure 16 ADAPT/CRISP Adaptation Method at 1 Body Length below SLSLE Process Started with Grid Using Best Method from Sourcing Study

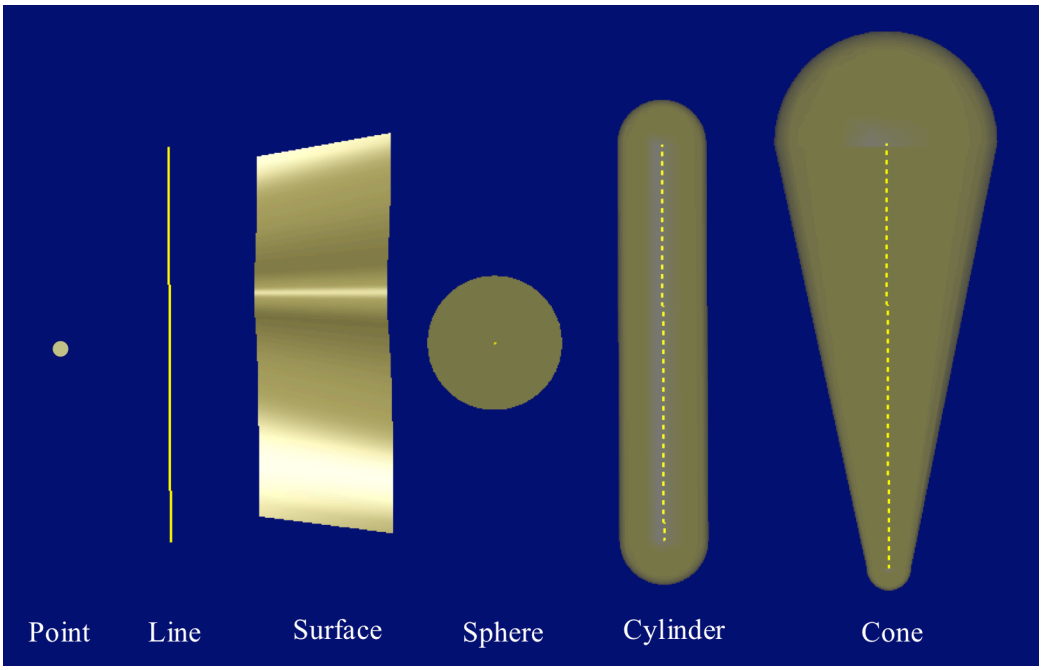

Figure 17 Source Types Available in VGRID

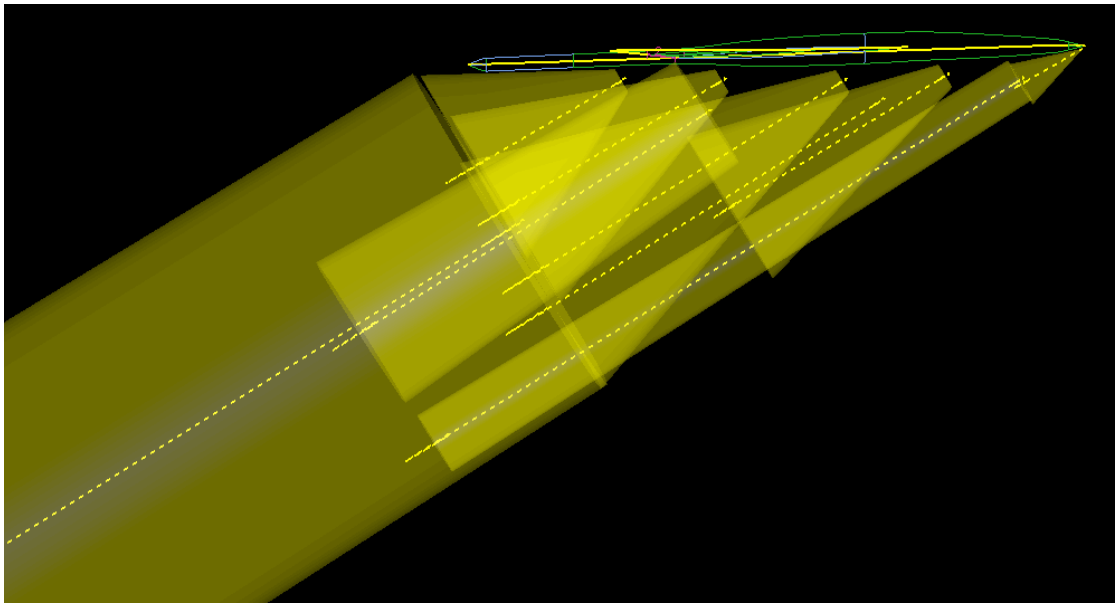

Figure 18 Volume Sources Underneath the SLSLE Configuration

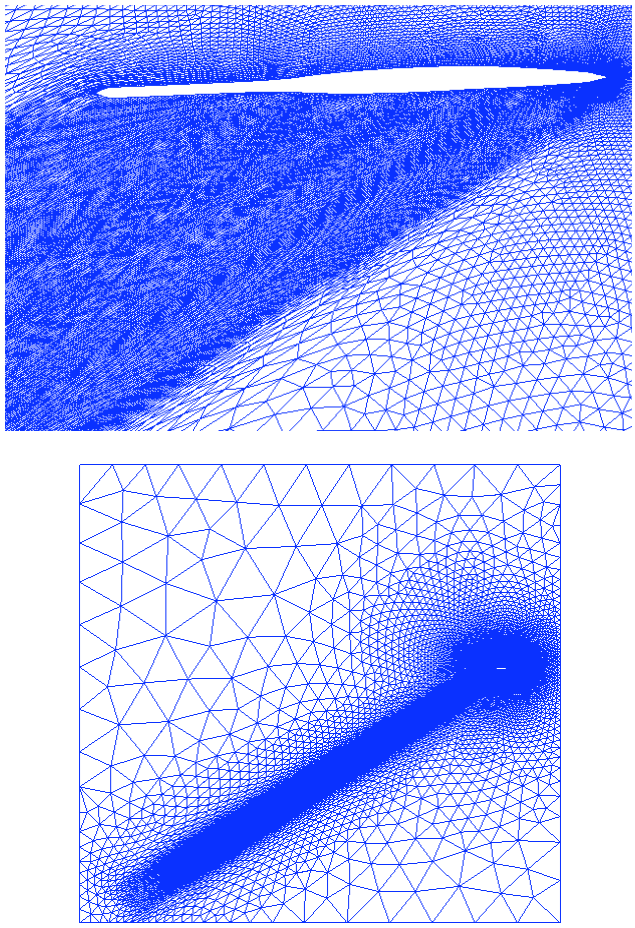

Figure 19 Grid Produced using Volume Sources on the SLSLE Configuration

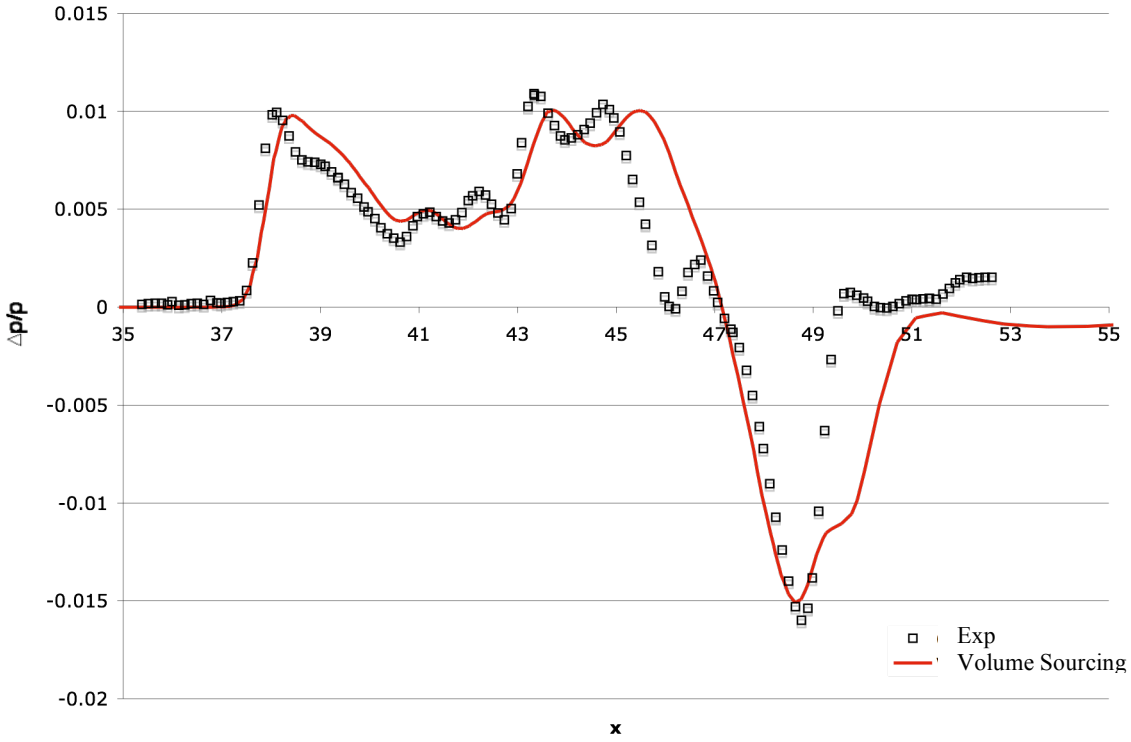

a) 2.5 Body Length Below SLSLE

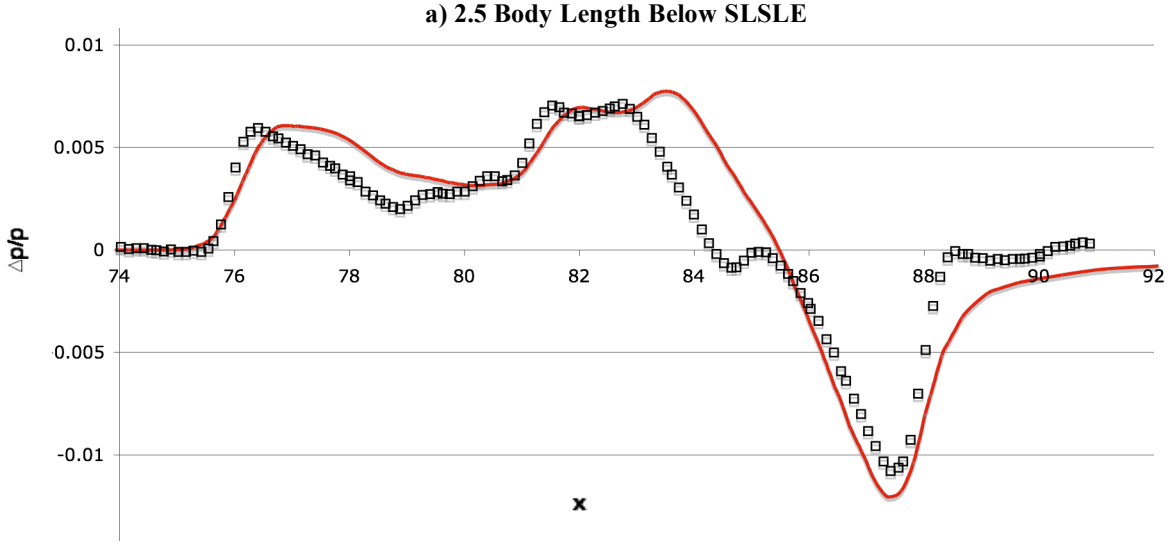

b) 5 Body Lengths Below SLSLE

Figure 20 Comparison of Δp/p on SLSLE using Volume Sourcing

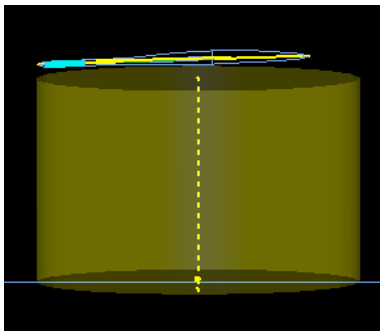

Figure 21 Single Volume Source Under SLSLE

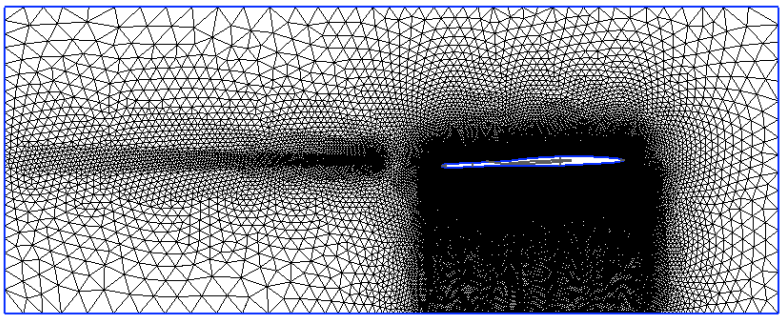

Figure 22 Initial Grid Produced for Input into SSGRID

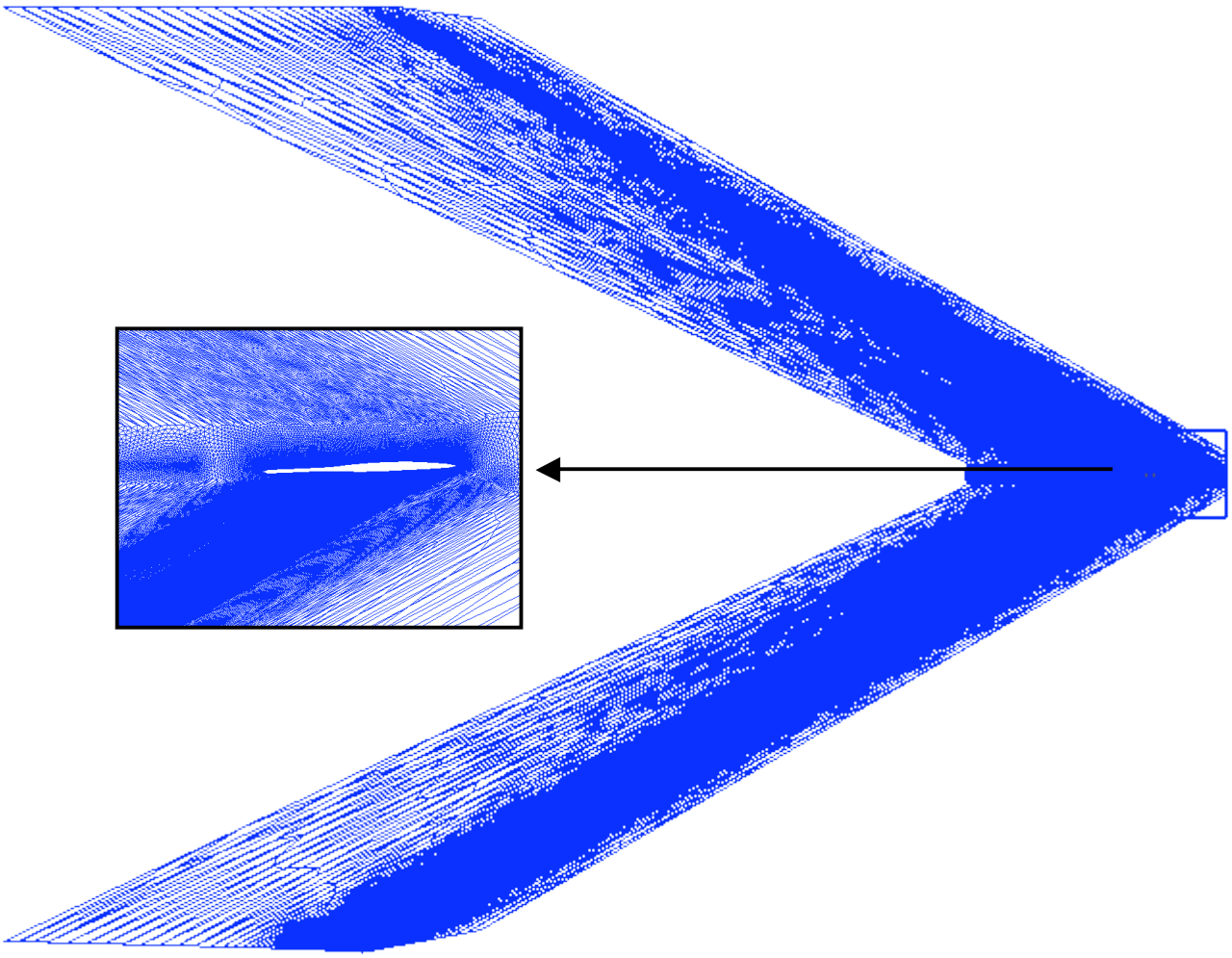

Figure 23 Sheared and Stretched Grid from SSGRID

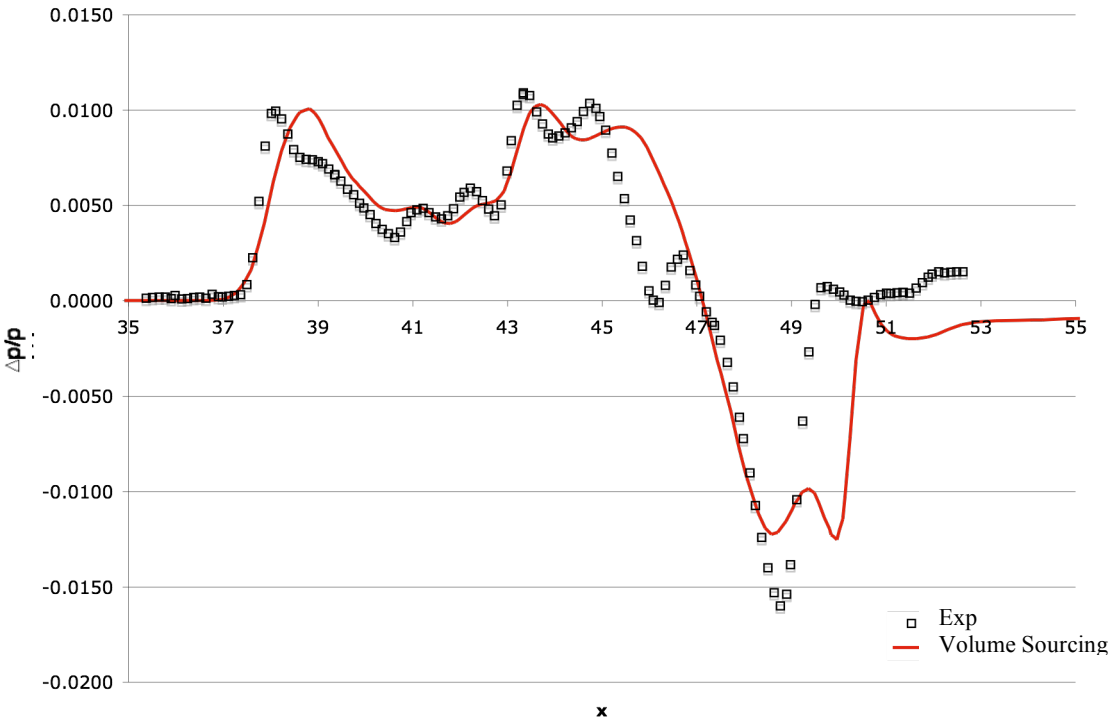

Figure 24 Comparison of Δp/p at 2.5 Body Lengths Below SLSLE using SSGRID

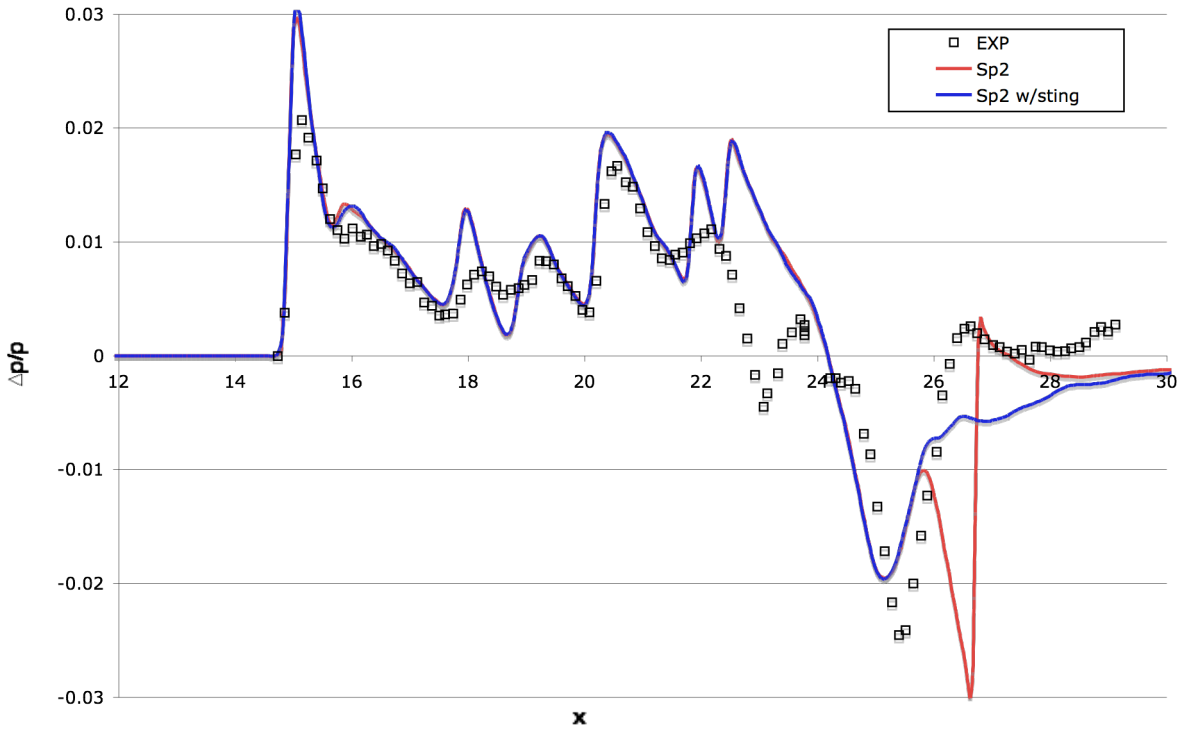

Figure 25 Comparison of the Effects of Modeling the Sting on Delta P/P at 1 Body Length Below SLSLE using SSGRID

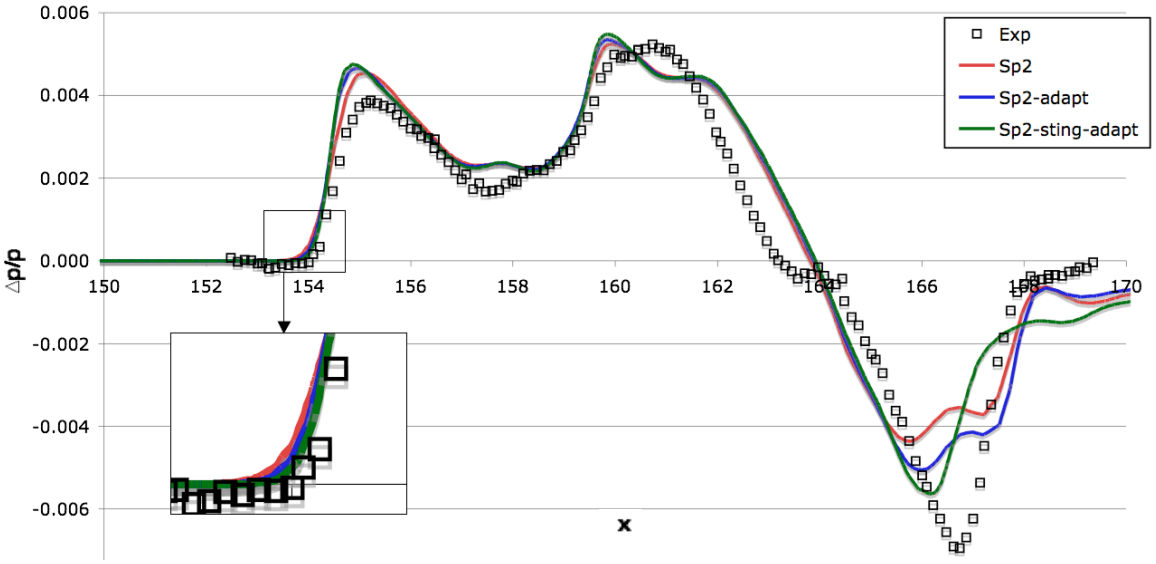

Figure 26 Comparison of the Effects of Adaptation on Delta P/P at 10 Body Length Below SLSLE using SSGRID

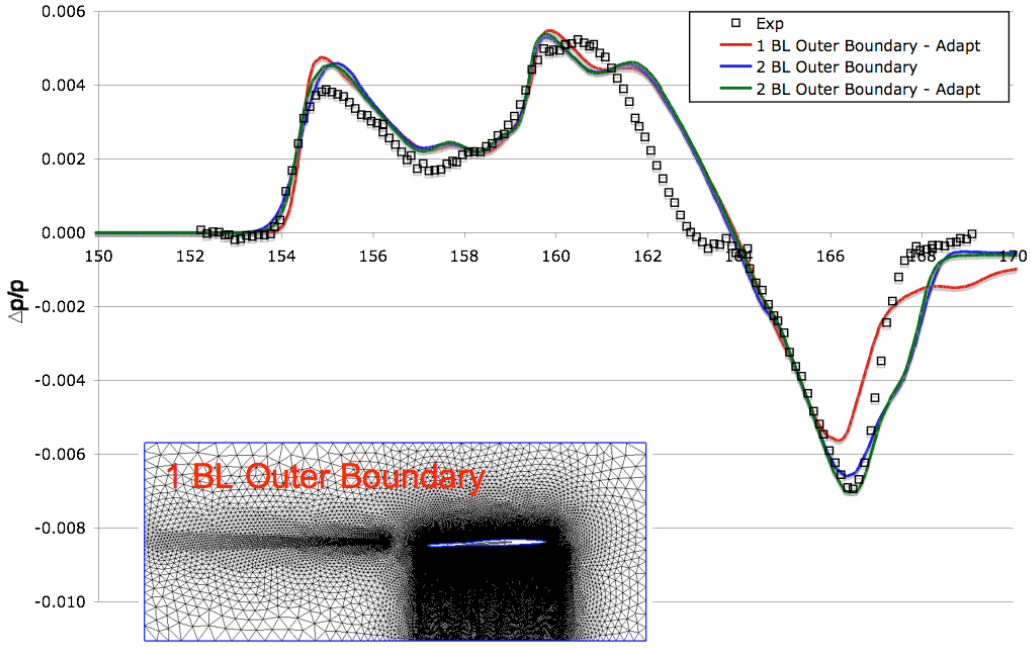

Figure 27 Comparison of the Effects of Outer Boundary Si n Delta P/P at 10 Body Length Below SLSLE using SSGRID

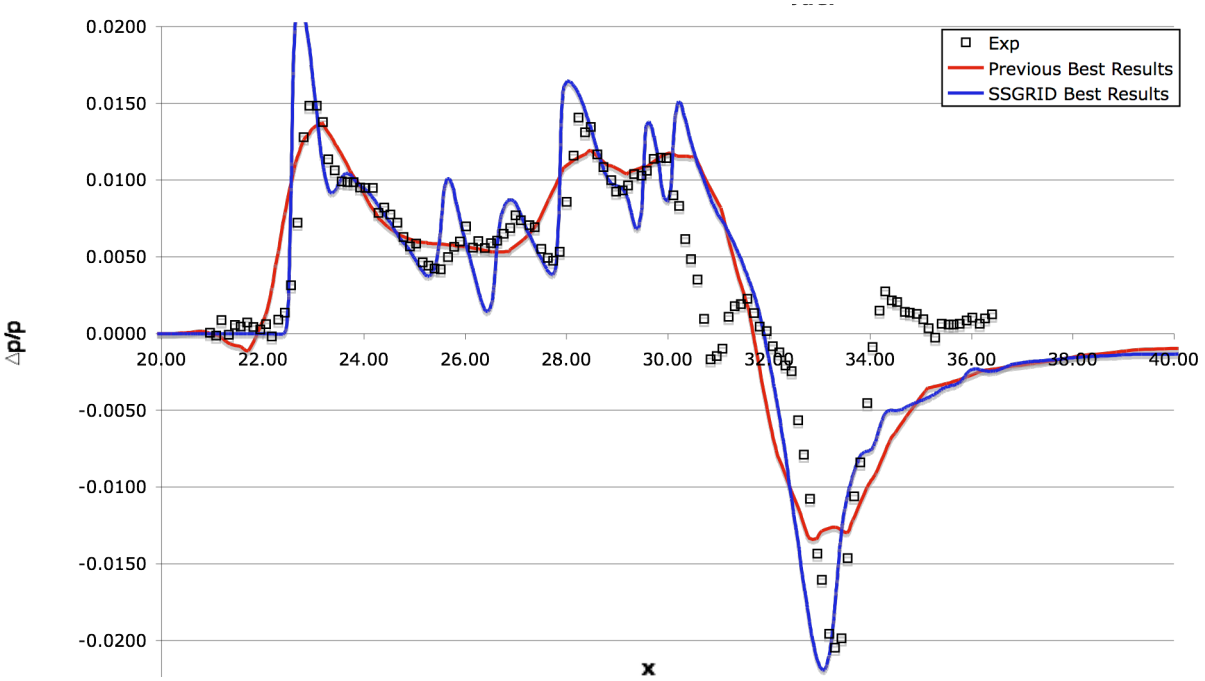

Figure 28 Comparison of the Best Results of CFD Prediction at 1.5 Body Lengths Below the Model

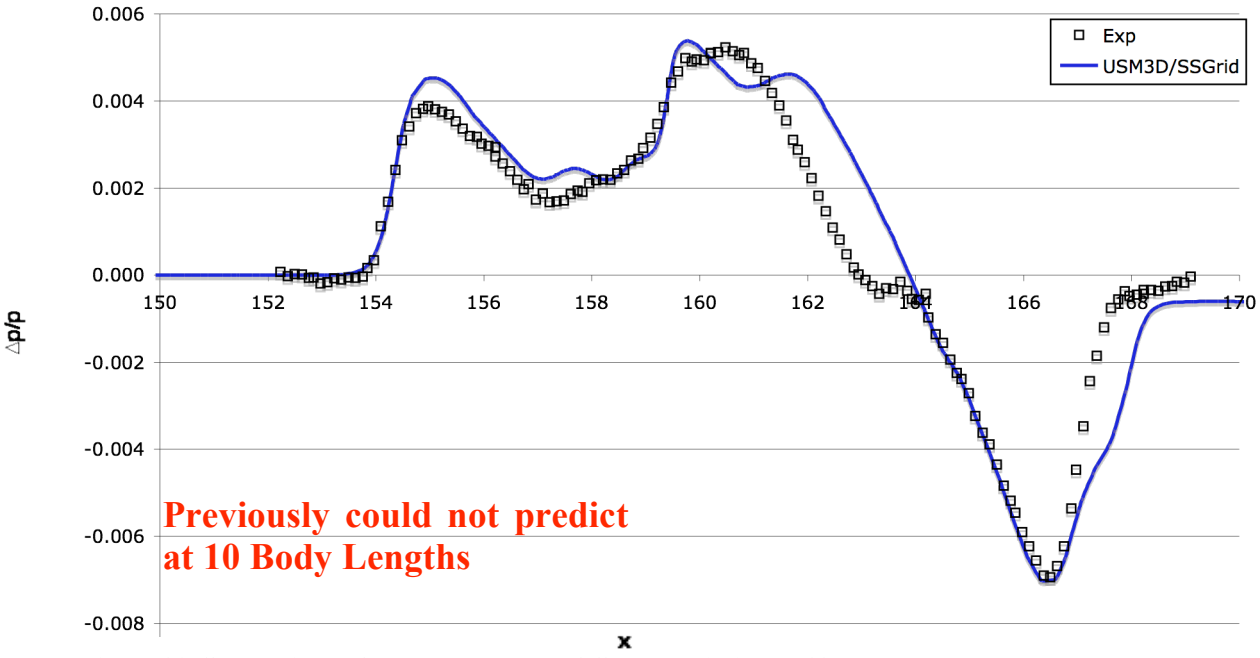

Figure 29 Comparison of the Best Results of CFD Prediction at 10 Body Lengths Below the Model